

Effect of Cross-Linkers on the Processing of Lignin/Polyamide Precursors for Carbon Fibres

Baljinder K. Kandola ^{1,*}, Trishan A. M. Hewage ^{1,2}, Muhammed Hajee ¹ and A. Richard Horrocks ¹

¹ Institute for Materials Research and Innovation, University of Bolton, Bolton BL3 5AB, UK

² Colorplas Ltd., Moss Bridge Road, Rochdale, Lancashire OL16 5PQ, UK

* Correspondence: b.kandola@bolton.ac.uk; Tel.: +44-1204-903517

Abstract: This work reports the use of cross-linkers in bio-based blends from hydroxypropyl-modified lignin (TcC) and a bio-based polyamide (PA1010) for possible use as carbon fibre precursors, which, while minimising their effects on melt processing into filaments, assist in cross-linking components during the subsequent thermal stabilisation stage. Cross-linkers included a highly sterically hindered aliphatic hydrocarbon (Perkadox 30, PdX), a mono-functional organic peroxide (Triganox 311, TnX), and two different hydroxyalkylamides (Primid[®] XL-552 (PmD 552) and Primid[®] QM-1260 (PmD 1260)). The characterisation of melt-compounded samples of TcC/PA1010 containing PdX and TnX indicated considerable cross-linking via FTIR, DSC, DMA and rheology measurements. While both Primids showed some evidence of cross-linking, it was less than with PdX and TnX. This was corroborated via melt spinning of the melt-compounded chips or pellet-coated TcC/PA1010, each with cross-linker via a continuous, sub-pilot scale, melt-spinning process, where both Primids showed better processability. With the latter technique, while filaments could be produced, they were very brittle. To overcome this, melt-spun TcC/PA1010 filaments were immersed in aqueous solutions of PmD 552 and PmD 1260 at 80 °C. The resultant filaments could be easily thermally stabilised and showed evidence of cross-linking, producing higher char residues than the control filaments in the TGA experiments.

Keywords: lignin; polyamide; cross-linker; blends; filaments; precursor; thermal stabilisation

Citation: Kandola, B.K.; Hewage, T.A.M.; Hajee, M.; Horrocks, A.R. Effect of Cross-Linkers on the Processing of Lignin/Polyamide Precursors for Carbon Fibres. *Fibers* **2023**, *11*, 16. <https://doi.org/10.3390/fib11020016>

Academic Editors: Ahmad Rashed Labanieh and Vincent Placet

Received: 12 December 2022

Revised: 8 January 2023

Accepted: 16 January 2023

Published: 29 January 2023



Copyright: © 2023 by the authors. Licensee MDPI, Basel, Switzerland. This article is an open access article distributed under the terms and conditions of the Creative Commons Attribution (CC BY) license (<https://creativecommons.org/licenses/by/4.0/>).

1. Introduction

While carbon fibres are very popular in lightweight structural composites used in the aerospace industry, in the automotive and construction industries, their growth in usage is limited by their high cost, which is partly due to the cost of production of the precursor fibre, namely, polyacrylonite (PAN). Hence, there is considerable interest in generating carbon fibres from alternative precursors [1–5]. One such is lignin, which is a relatively low-cost by-product of the paper and pulp industry and is a potential candidate because of its high carbon content (60–65%) [6–8]. With some simple chemical modifications (e.g., organosolv or kraft) [1,9], lignin can be melt spun into fibres. However, continuous melt spinning of lignin is not easy unless it is blended with some other thermoplastic polymer that is mainly used as a carrier material [9–11]. The miscibility of the blended polymers is important for the production of void-free, good-quality precursor filaments [9,12]. Another important criterion is the melting/processing temperature of the carrier polymer, which should be low enough to avoid thermal degradation of the lignin, which generally occurs at approximately 190–200 °C [13]. However, such thermally induced depolymerisation of lignin can lead to the production of volatiles, which can form defects/voids within the resulting lignin fibre structure. Moreover, the accompanying polycondensation reactions can impede the melt-flow characteristics of the lignin, which can have an adverse effect on the melt-extrusion process. Whilst the melt spinning of lignin

blended with many polymers was reported, such as with polyethylene (PE) and polyethylene oxide (PEO) [11], polyvinyl alcohol (PVA) [14], polyethylene terephthalate (PET) [15], polypropylene (PP) [15], polyamides [9,16] and TPU [17], very few of these procedures included spinning blends into continuous filaments at a pilot scale. In this context, we reported the production of continuous fibres from an organosolv hardwood lignin (TcC) and the bio-polyamides 1010 (PA1010) and 1012 (PA1012). The derived blends had good compatibility and the resulting filaments showed good mechanical properties [9,16].

Having secured acceptable lignin/bio-polyamide blended filaments, the next challenge was to thermally stabilise them prior to their final carbonisation into carbon fibres with acceptable mechanical properties. During thermal stabilisation, the cross-linking of adjacent lignin-lignin, lignin-biopolyamide and even biopolyamide-biopolyamide chains is required to convert the thermoplastic blend components into a thermoset composite structure, thereby ensuring that filaments do not fuse together during the subsequent high-temperature carbonisation stage. In the case of conventional carbon fibre production, the PAN precursor filaments are usually thermally stabilised under air at 200–300 °C for about 1.5 h and then slowly cooled to room temperature (e.g., a circa 5 °C/min cooling rate) such that the whole process takes ~2.5 h [18]. However, lignins were shown to require very slow heating rates (0.1–2 °C/min) to temperatures in the region of 200–300 °C for several hours in order to cross-link sufficiently, and thus, avoid fusion during subsequent higher-temperature carbonisation [19–21]. This stabilisation process may be significantly slowed further when a thermoplastic polymer is co-blended with the lignin since typical examples, such as polyamides, polyesters and polyolefins, do not readily auto-cross-link. Thus the cross-linking required to take place during the stabilisation of a lignin blend may be difficult to achieve unless a cross-linking agent is added to one or both blend components. Cross-linking agents can interconnect long chains of the two polymers by forming covalent bonds between them, either by generating free radicals, which can abstract an H atom from the polymer backbone, and thus, activate adjacent chains, or by acting as a bridge between functionalities within them. For the latter, cross-linkers with bifunctional or multifunctional molecules with the ability to react with specific functional groups (amines, carboxyl, carbonyl, hydroxyl, etc.) of each polymer are required. Recent reports of the use of such cross-linking agents include the introduction of boric acid and dicumyl peroxide (which involve both approaches, with boric acid forming bridges and dicumyl peroxide forming free radicals) to develop multiphase networks between a hardwood soda lignin and a softwood Kraft lignin blended with acrylonitrile butadiene rubber [22], maleic anhydride as a coupling agent (similar to cross-linkers, forming covalent bonds between two components) in lignin-polypropylene blends [23], a proprietary cross-linking agent present in maleic-anhydride-compatibilised poly(lactic acid)/polyamide 11 blends [24] and dicumyl peroxide to cross-link an ethylene–vinyl acetate copolymer with polyamide 12 (PA12) through free radical reactions [25]. In some of these examples, the mechanical properties of the blends/fibres were also improved.

The aim of this work was to explore the use of different cross-linking agents in organosolv hardwood lignin (TcC)/bio-polyamide (PA1010) blends, which we previously demonstrated may be melt extruded into filaments with acceptable mechanical properties, and thus, render them more suitable for subsequent stabilisation and carbonisation [9,12,16]. These previous studies showed that without any cross-linker addition, the thermal stabilisation of TcC/PA1010 filaments required slow heating rates (e.g., 0.25 °C/min), which were similar to those reported in the literature for lignin-based fibres [19–21]. The addition of compatibilisers, such as the terpolymers ethylene-methyl acrylate-glycidyl methacrylate and ethylene-acrylic ester-maleic anhydride, whilst improving the blend homogeneity and filament mechanical properties, had a minimal effect on the thermal stabilisation stage [16], hence the need to use cross-linking agents in the present work. The cross-linking agents selected included, first, 2,3-dimethyl-2,3-diphenylbutane as an example of a highly sterically hindered aliphatic hydrocarbon that was expected to decompose homolytically at temperatures >200 °C and a mono-functional organic peroxide, both of

which can initiate radical cross-linking reactions. Second, examples of two different hydroxyalkylamide cross-linkers commonly used in the polymer-coating industries were used. Cross-linking agents were introduced directly into polymer blends via melt compounding, blended polymer pellet-coating immediately prior to filament extrusion or adsorption using freshly extruded filaments from aqueous cross-linker solutions. The characterisation of the resulting filaments was undertaken using thermal analytical, rheological, mechanical and morphological methods. The resulting filaments were then thermally stabilised under varying conditions and characterised.

2. Materials and Methods

2.1. Materials

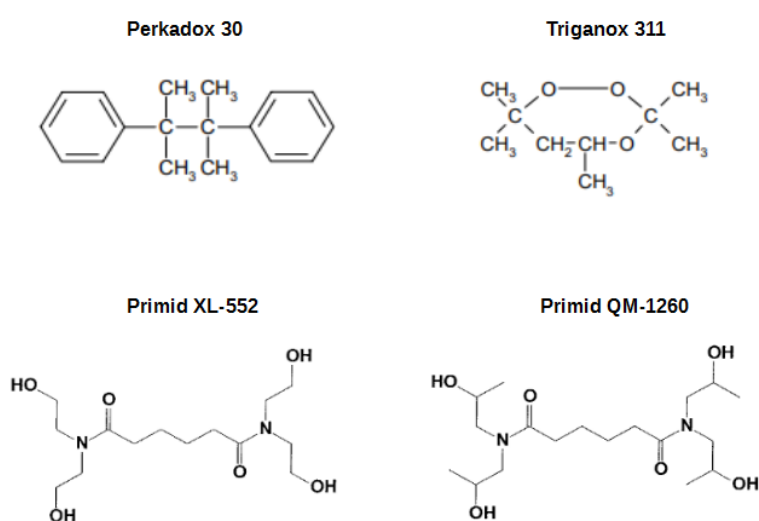
An organosolv hardwood lignin, namely, TcC (M_w : 11,357 g/mol and PDI: 4.58), was sourced from Tecnaro, Ilsfeld, Germany. A detailed characterisation of this lignin is reported elsewhere [26]. A bio-based polyamide 1010 (PA1010, 3960R) was supplied by Evonik Industries, Germany. The following cross-linkers were selected for this work.

Perkadox 30 (PdX), 2,3-dimethyl-2,3-diphenylbutane, commonly used as an initiator for the polymerisation of styrene, sourced from Nouryon (previously Akzo Nobel). It was expected that Perkadox 30 would decompose homolytically at high temperature (1 h half-life at 259 °C [27]) and initiate radical crosslinking reactions.

Triganox 311 (TnX), 3,3,5,7,7-pentamethyl-1,2,4-trioxepane, a monofunctional organic peroxide supplied by Nouryon (previously Akzo Nobel). This is typically used to cross-link natural rubbers, as well as thermoplastic polyolefins. The typical cross-linking temperature of Triganox 311 (1 h half-life at 166 °C [27]) is within the processing range for TcC/PA1010 processing, and hence, is expected to be an effective cross-linker.

Primid® XL-552 (PmD 552) and Primid® QM-1260 (PmD 1260), both hydroxyalkylamide cross-linkers, sourced from Ems-Griltech AG, Domat/Ems, Switzerland. PmD 552 (M. Pt.: 120–125 °C), with hydroxy value 620–700 mgKOH/g [28], was expected to be more reactive than PmD 1260 (M. Pt.: 100–115 °C, 550–650 mgKOH/g [29]). Both of these cross-linkers start curing above 165 °C and are typically used in durable powder coatings for exterior use. These were also reported to be used for the cross-linking of polyamides [30].

The chemical structures of all cross-linkers are reported in Scheme 1.



Scheme 1. Chemical structures of the cross-linking materials.

2.2. Melt Compounding and Melt Spinning into Continuous Filaments

Different formulations were prepared via hand-mixing 50 wt% TcC and 50 wt% PA1010 in a plastic container, to which cross-linkers were added in varying amounts (see Table 1). Each mixture was stirred using a glass rod to ensure homogeneity of the blend and then dried in an oven at 85 °C for 2 h prior to compounding. A twin-screw extruder (ThermoFisher Scientific™ Prism Eurolab 16, Swindon UK) with a screw rotation speed of 100 rpm was used to produce lignin/polyamide blends. The blends were processed with temperature profiles over six heating zones varying between 180 and 190 °C. The compounded coarse strands were passed through a water bath before being pelletised. The composition of all melt-compounded blends and the ease of processability are summarised in Table 1.

Table 1. Sample composition and the ease of processability during compounding.

Sample	Cross-Linker in TcC/PA1010 50:50 wt%		Processability
	Type	Conc (pph)	
TcC/PA1010	-	-	Easy
TcC/PA1010/PdX-1	Perkadox 30	1	Moderate
TcC/PA1010/PdX-2	Perkadox 30	2	Moderate
TcC/PA1010/PdX-3	Perkadox 30	3	Moderate
TcC/PA1010/TnX-1	Triganox 311	1	Moderate
TcC/PA1010/TnX-2	Triganox 311	2	Difficult
TcC/PA1010/TnX-3	Triganox 311	3	Difficult
TcC/PA1010/PmD552-1	Primid XL-552	1	Easy
TcC/PA1010/PmD552-5	Primid XL-552	5	Easy
TcC/PA1010/PmD552-10	Primid XL-552	10	Moderate
TcC/PA1010/PmD1260-1	Primid QM-1260	1	Easy
TcC/PA1010/PmD1260-5	Primid QM-1260	5	Easy
TcC/PA1010/PmD1260-10	Primid QM-1260	10	Moderate

Note: pph—parts per hundred of the polymer blend.

A single-screw melt extruder (Labline MK 1) was used to extrude filaments from TcC/PA1010/cross-linker blended pellets. Pellets were oven-dried at 85 °C overnight prior to melt extruding into filaments. This small yet versatile extruder is capable of extruding filaments from polymers and blends that are often considered to be difficult to extrude compared with more sophisticated extruders, hence its use. As small quantities of pellets were required during the spinning trials (typically ~250 g), the wastage of material was also minimal using this extruder. The internal diameter and aspect ratio of the screw were 22 mm and 20, respectively. A 40-hole spinneret (orifice diameter 0.5 mm) was used during the filament extrusion with a barrel temperature profile of 180–200 °C. The screw speed was maintained between 30 and 50 rpm, while slow and fast collection rolls were maintained at 10 and 20 m/min, respectively, imparting a nominal 2:1 stretch ratio.

TcC/PA1010/cross-linker blends could not be easily extruded into useful filaments. This was because most of the cross-linkers had decomposition or reactivity temperatures within the melt compounding and subsequent melt extruder temperature range of 180–200 °C, and thus, partial cross-linking occurred during both processes.

In order to minimise the partial cross-linking reactions during the compounding and extrusion, it was decided to introduce the cross-linking agents during the post-compounding stage using a pellet-coating method. Therefore, small quantities (≤ 0.5 wt%) of each cross-linker were added to the compounded TcC/PA1010 blend pellets and mixed thoroughly in a plastic container prior to being introduced to the filament extrusion process. Using this method, it was possible to produce useful filaments and their spinnability and quality are subjectively summarised in Table 2, with supporting images shown in

Figure 1. These samples are identified by the suffix “PC” (pellet-coated) in Table 2 and Figure 1.

Table 2. Summary of the ease of TcC/PA1010_50:50 filament extrusion and resulting filament character using the pellet-coating method.

Sample	Spinnability	Brittleness/Strength
TcC/PA1010	Good	Strong
TcC/PA1010/PdX-0.5_PC	Poor	Very brittle
TcC/PA1010/TnX-0.5_PC	Good	Strong
TcC/PA1010/PmD552-0.5_PC	Good	Strong
TcC/PA1010/PmD1260-0.5_PC	Good	Strong

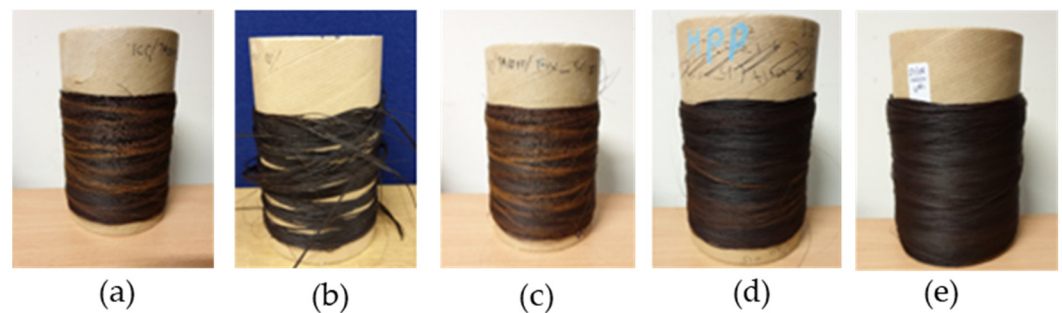


Figure 1. Images of continuously spooled filaments from TcC/PA1010_50:50 pellets using the pellet-coating method: (a) TcC/PA1010, (b) TcC/PA1010/PdX-0.5_PC, (c) TcC/PA1010/TnX-0.5_PC, (d) TcC/PA1010/PmD552-0.5_PC and (e) TcC/PA1010/PmD1260-0.5_PC.

2.3. Characterisation of Compounded Pellets

Fourier-transform infrared–attenuated reflection spectroscopy (FTIR-ATR) was conducted on melt-blended pellets using a Thermo Scientific Nicolet 6700 FTIR instrument with a Smart iTR attachment fitted with a single reflection diamond crystal. The spectra were recorded between 4000 and 400 cm^{-1} , each with 32 scans and a 4 cm^{-1} resolution.

Differential scanning calorimetry (DSC) was performed using a TA Q2000 (TA Instruments, Wilmslow, UK) under a nitrogen atmosphere (50 mL/min) with a sample size of about 3 mg. All samples were subjected to heat–cool–heat cycles with the first heating cycle being performed from 0 to 250 $^{\circ}\text{C}$ at 10 $^{\circ}\text{C}/\text{min}$. The samples were then cooled to 0 $^{\circ}\text{C}$ at a 5 $^{\circ}\text{C}/\text{min}$ cooling rate. Subsequently, the second heating cycle was performed up to 250 $^{\circ}\text{C}$ at 10 $^{\circ}\text{C}/\text{min}$. Only the first cooling and second heating cycles are reported in this work, as the aim of the first heating cycle was to eradicate the effects of the thermal processing history on the samples.

The glass transition temperature (T_g) of each sample was determined using dynamic mechanical analysis (DMA; TA instruments Q800 DMA). Approximately 2 g pellet specimens of each sample were sandwiched between rigid aluminium plates (thickness: 0.6 mm) and then a thin aluminium foil (thickness: 0.05 mm) was wrapped around them to avoid sample loss during the experiment. The $\tan \delta$ peak was considered as the second-order thermal transition (T_g) of each sample. The measurements were performed in a single cantilever mode from room temperature to 140 $^{\circ}\text{C}$ with a heating rate of 3 $^{\circ}\text{C}/\text{min}$, 1 Hz frequency and an oscillation amplitude of 15 μm .

The rheological properties were assessed using a Discovery Hybrid Rheometer HR2 equipped with an environmental control chamber (TA instruments, UK) using specimens that were approximately 2 g. Samples were subjected to dynamic frequency sweeps at 200 $^{\circ}\text{C}$ in a parallel-plate geometry with a plate diameter of 25 mm. The gap between the parallel plates was 1 mm. For all the samples, a 2% constant strain was used to perform experiments over the frequency range of 628 to 0.1 rad/s.

The thermal stabilities of the samples were studied via thermogravimetry (TGA) using an SDT-Q600 instrument (TA instruments, UK) under a flowing nitrogen atmosphere (100 mL/min) with a heating rate of 20 °C/min from 30 to 900 °C. The sample sizes used were 8–10 mg.

2.4. Characterisation of Melt-Spun Filaments from Pellet-Coated Blends Regarding Mechanical and Morphological Properties

Morphologies of filaments were studied using a Hitachi S-3400 N scanning electron microscope (SEM) with a beam voltage of 5 kV. The filaments were frozen at −8 °C for 4 h before fracturing them to provide clean cross-sections for analysis. All the samples were gold sputtered before morphological investigations were conducted.

Tensile properties of the filaments were determined using an Instron-3369 tensile instrument and a 1 kN load cell at a cross-head speed of 50 mm/min with a gauge length of 100 mm. The diameters of filaments were measured from the SEM images as averages of five measurements per specimen. The reported values of tensile properties were averaged values of at least five repeat tests.

2.5. Pre-Treatment of TcC/PA1010 with Cross-Linkers and Thermal Stabilisation

As an alternative process to adding cross-linkers during compounding, the extruded TcC/PA1010 filaments were impregnated with aqueous solutions of the water-soluble cross-linking agents PmD 552 and PmD 1260.

2.5.1. Filament Extrusion and Immersion

For this work, TcC/PA1010 filaments were produced using a Fibre Extrusion Technology Ltd. (FET-101, Leeds, UK) extruder. The filament spinnerette had 24 holes, each with an orifice diameter of 0.8 mm. The extruder screw (internal diameter of 21 mm with L/D = 30:1 and screw speed of 25 rpm) comprised four different temperature zones ranging from 185 to 195 °C and a metering pump/spinnerette zone at 215 °C.

For impregnation with cross-linkers, 500 mL aqueous solutions containing 0.5 and 1.0 wt.% of both PmD 552 and PmD 1260 were prepared. These levels were determined based on the results of melt-blended and pellet-coated blends. The beaker containing each solution was heated at 80 °C for 1 h to reach a temperature above that of the blended filament's glass transition temperature. Then, 30 cm length cut samples (as 10 fibre bundles) were clamped at a constant length horizontally in a ceramic tray before being submerged in the hot prepared solution, as shown schematically in Figure 2. The whole assembly was placed in an oven at 80 °C for 1 h. After this, the precursor filament lengths were removed from the oven and tray and left to dry at room temperature for 2 h. Filament bundle specimens were washed with distilled water to remove any residual Primid cross-linking agent remaining on the surface and left to dry in the laboratory overnight.

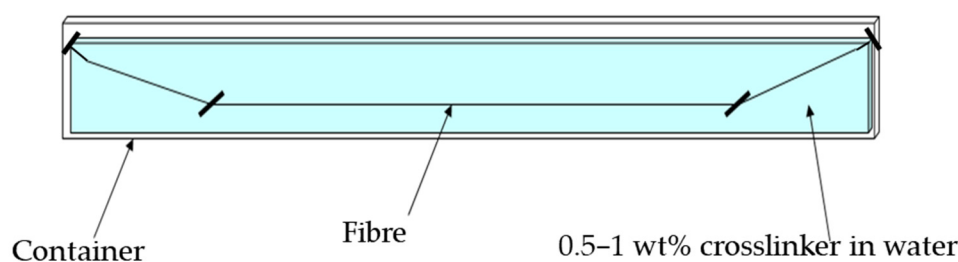


Figure 2. Schematic representation of TcC/PA1010 filaments immersed in aqueous solutions of cross-linkers.

2.5.2. Thermal Stabilisation

Untreated and cross-linking agent-treated TcC/PA1010 filaments were thermally stabilised using a laboratory oven (Leader Engineering, London, UK) equipped with a programmable Eurotherm 3216 proportional–integral–derivative (PID) controller. The filament precursor bundles of 30 cm in length were held together using thermal tape on either end. The filament bundles were hung vertically and fastened to an oven rack using this tape. An optimal, known weight (2 g) of steel paper clips was suspended from the lower bundle ends to introduce tension to the vertically orientated bundles. This 2 g weight was determined using trial experiments on TcC/PA1010 filaments, where it was observed that a 1 g weight was insufficient for the fibres to be elongated and a 3 g weight snapped the fibres; however, a 2 g weight caused the fibre bundles to be extended almost to the maximum length of the oven chamber while maintaining tension. Thermal stabilisation was conducted at two different temperatures (180 °C and 250 °C) in sequence under atmospheric conditions. In the first step, the filaments were isothermally stabilised at 180 °C for 1 h after being heated from room temperature to 180 °C with a heating rate of 0.25 °C/min. At this temperature, which was close to the filament melting point, it was assumed that cross-linking reactions would be initiated and would be sufficient to enable the fibres to be raised to 250 °C for full stabilisation based on the respective cross-linker information. Subsequently, the filaments were heated to 250 °C with a heating rate of 0.25 °C/min and kept at 250 °C for 2 h to thermally stabilise them. Thus, while the temperatures for this two-stage stabilisation were based on these respective thermal conditions, the stabilisation time was determined using trial experiments.

The mechanical properties of the thermally stabilised filaments were assessed as explained in Section 2.4

3. Results

3.1. Effect of Cross-Linkers on Physico-Chemical Changes in Lignin/PA1010 Blends (Melt Compounded)

3.1.1. FTIR Spectroscopic Analysis

In order to identify any cross-linking occurring during the melt-processing stage of the blends (see Section 2.2), the compounded blends were investigated using FTIR spectroscopy. Figure 3 shows the FTIR spectra of TcC/PA1010 and blends containing 1 pph of PdX, TnX, PmD 552 and PmD 1260.

Detailed FTIR spectra of the PA1010, TcC and TcC/PA1010 blends were reported in earlier publications [9,12,16]. In brief, the spectrum of TcC/PA1010 showed peaks that are characteristic of both TcC lignin and PA1010, which were shifted slightly due to some intermolecular interaction compared with those in neat polymers, as observed previously. The characteristic peaks of the TcC component at 1715 cm^{-1} , assigned to aldehyde and carboxylic acid C=O groups, and at 1234 cm^{-1} , assigned to C-O-C ether bonds, can be seen in Figure 3, where the latter appears at 1231 cm^{-1} . The peaks at 1637 cm^{-1} could be assigned to the amide I (C=O) and 1538 cm^{-1} to amide II (N-H) groups of the polyamide component [9,12,16].

The spectra of TcC/PA1010 containing 1, 2 and 3 pph PdX and TnX comprised all the peaks seen in the unmodified TcC/PA1010 blend, but with more pronounced peaks at 1970, 2025 and 2156 cm^{-1} , respectively, which could be assigned to C-H bending in the first case and to unstable allene (C=C=C) and ketene (C=C=O) species in the second and third cases, respectively. While the two latter cases are difficult to explain, they do not provide evidence of cross-linking.

The cross-linking agent Perkadox 30 was reported to have a half-life of 1 h at 259 °C [27] and decomposes homolytically, and thus, was assumed here to initiate radical cross-linking reactions in the blend. Triganox 311 is a mono-functional organic peroxide with a half-life of 1 h at 166 °C [27], and thus, will also be expected to have promoted component interactions within the blend. However, blends containing PmD 552 and PmD 1260 are

expected to interact through their -OH groups with the -OH groups of lignin and the -NH₂ and carboxyl groups [30] of PA1010. Any such cross-links would be expected to form additional ether links, and while accepting the error within FTIR-ATR measurements, the expanded spectra in the 1100–1400 cm⁻¹ range in Figure 3b showed that relative to the 1257 cm⁻¹ peak (a probable amide III N-H bend vibration in PA1010), the intensity of that at 1231 cm⁻¹ (assigned to C-O-C ether bond) increased slightly, indicating some cross-linking reactions. This was also seen in the case of the PdX-containing sample.

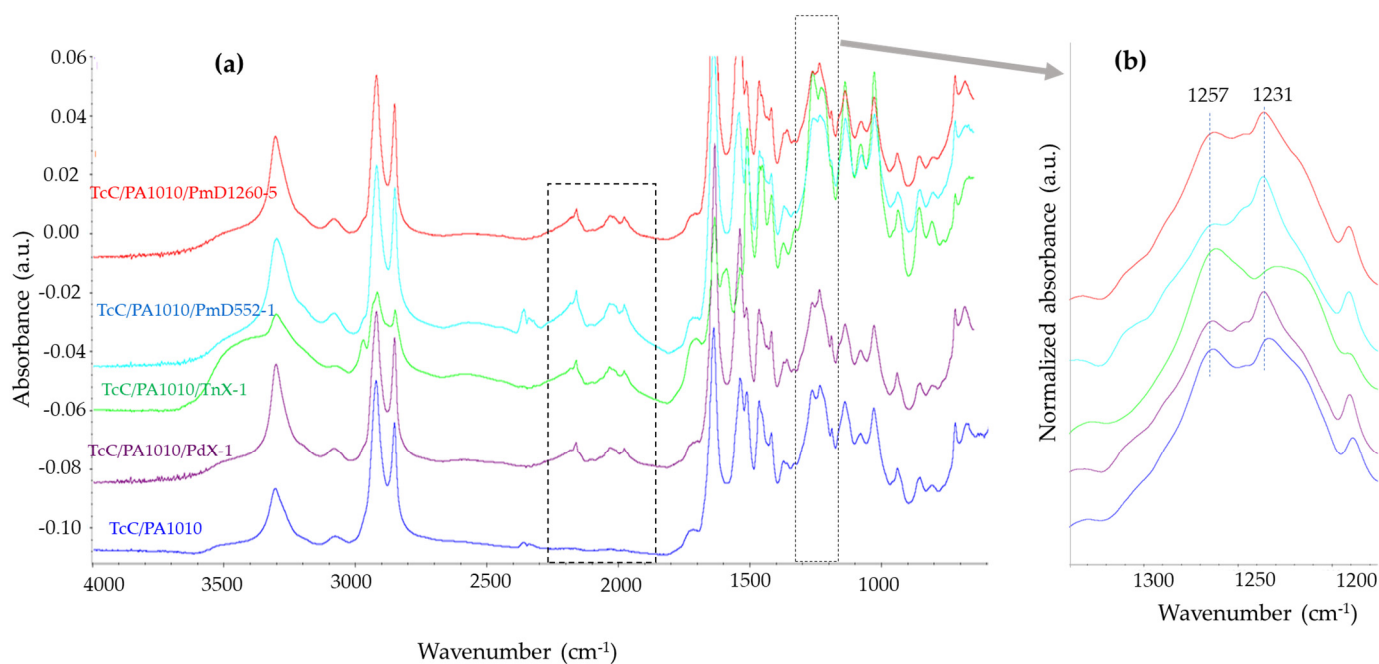


Figure 3. FTIR spectra of TcC/PA1010 and TcC/PA1010 blends containing PdX, TnX, PmD 552 and PmD 1260 cross-linkers: (a) 800–4000 cm⁻¹ and (b) 1100–1400 cm⁻¹ range.

3.1.2. Differential Scanning Calorimetric Analysis

The DSC traces of the TcC/PA1010 blended pellets with and without 1 pph cross-linkers are shown in Figure 4, and the data derived from these traces are summarised in Table 3. The second heating thermogram of the TcC/PA1010 control showed a bimodal endothermic peak, which was associated with bimodal melting points (T_m) of γ -crystalline (186 °C) and α -crystalline (197 °C) phases of PA1010 [9,16,31]. After the addition of PdX or TnX, the temperatures of both peaks reduced slightly (183–184 °C and 193–194 °C, respectively), suggesting heterogeneously nucleated crystallisation. However, the melt enthalpy (ΔH_m) increased with 1 pph PdX or TnX but decreased with increasing cross-linker contents, with it being minimal at the 3 pph level. The maximum crystallisation temperatures (T_c) of PA1010, which were derived from the first cooling curve, remained unaffected at 1 or 2 pph PdX levels but decreased after increasing to 3 pph PdX. However, the enthalpies of crystallisation (ΔH_c) increased with 1 and 2 pph PdX. The reduction in T_c of PA1010 in TnX-containing samples (171–172 °C) was greater than for the respective PdX-containing samples. The fact that the changes in ΔH_m values were not reflected in the respective ΔH_c values was probably a consequence of the annealing of the latter-formed crystals during the second heating scan. These decreases in melting and crystallisation temperatures represented the effects of cross-linking reactions. For these samples showing low-temperature cross-linking reactions, a greater difficulty was also observed during their melt spinnabilities, as reported in Table 2.

However, with PmD552 and PmD1260, there was minimal effect on the T_m and T_c values, particularly at the 1 pph levels. ΔH_m and ΔH_c were also lower than in the

TcC/PA1010 control (except for the T_m value of TcC/PA1010/PmD, which could be an experimental error), which seemed to be independent of the cross-linker content level. The absence of any notable effect suggested that the Primid agents appeared to have a minimal effect on cross-linking the lignin and PA1010 components.

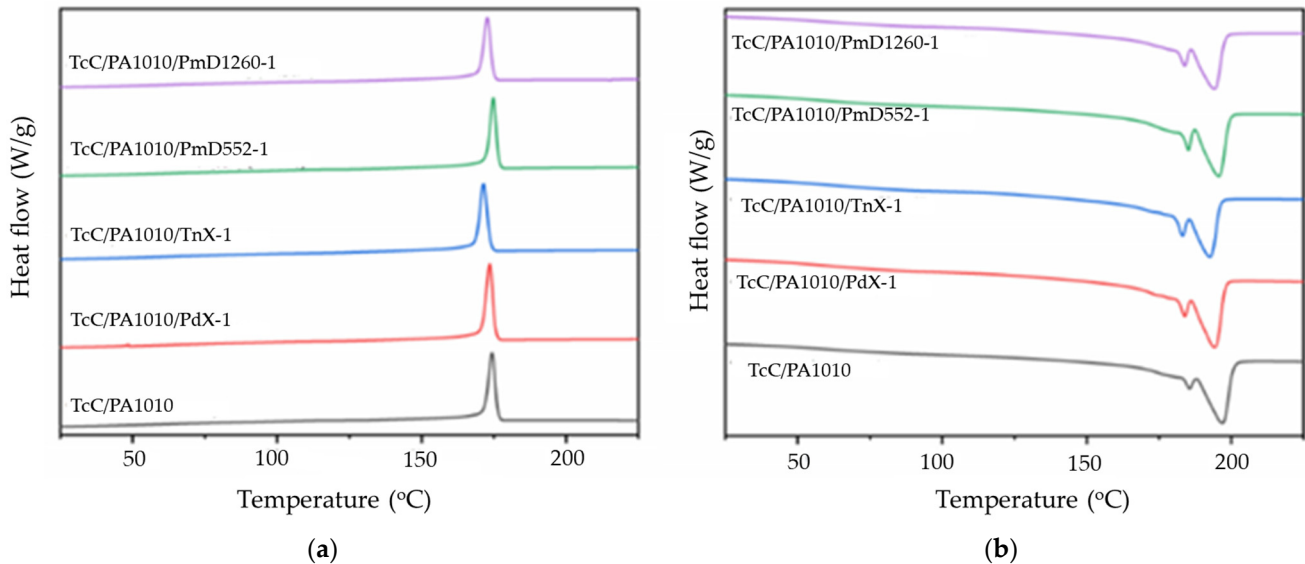


Figure 4. DSC thermograms of TcC/PA1010 blends in the presence and absence of cross-linkers: (a) first cooling and (b) second heating scans.

Table 3. Thermophysical transitions from the DSC and DMA, and thermochemical transitions from the TGA responses of TcC/PA1010 with and without cross-linkers.

Samples	DSC				DMA		TGA	
	T_m (°C)	ΔH_m (J/g)	T_c (°C)	ΔH_c (J/g)	T_g (°C)	T_{Onset} (°C)	T_{Max} (°C)	CY* at 880 °C (%)
TcC/PA1010	186,197	33.6	174	34.6	68, 146	337	457	19 (17.0)
TcC/PA1010/PdX-1	184,194	37.7	174	35.2	*, 147	328	458	19 (16.8)
TcC/PA1010/PdX-2	184,194	35.3	174	37.5	*, 145	317	456	20 (16.7)
TcC/PA1010/PdX-3	183,193	33.8	172	34.8	*, 144	299	454	18 (16.5)
TcC/PA1010/TnX-1	183,193	34.4	171	35.1	*, 146	331	449	19 (17.0)
TcC/PA1010/TnX-2	184,193	33.8	172	34.1	*, 145	311	456	18 (16.7)
TcC/PA1010/TnX-3	183,193	32.5	171	33.9	*, 146	310	449	21 (16.5)
TcC/PA1010/PmD552-1	185,196	35.9	175	33.6	66, 152	322	412	24 (16.8)
TcC/PA1010 /PmD552-5	186,195	28.6	175	27.8	67, 126	330	447	23 (16.2)
TcC/PA1010/PmD552-10	187,194	26.6	175	26.4	68, 109	325	452	21 (15.3)
TcC/PA1010 /PmD1260-1	184,194	33.1	173	31.3	68, 150	322	416	23 (16.8)
TcC/PA1010/PmD1260-5	185,195	32.6	173	29.8	69, 134	325	455	19 (16.2)
TcC/PA1010/PmD1260-10	187,195	28.9	174	29.1	70, 112	306	441	21 (15.3)

* No defined peak observed; the values in parentheses and italics are the calculated expected sums of those from the individual components.

3.1.3. Dynamic Mechanical Analysis (DMA)

DMA provides higher sensitivity when measuring the glass transition T_g than DSC because DMA directly measures changes in mechanical and viscoelastic properties as a function of temperature rather than small changes in heat capacity, and hence, it was used to measure the T_g values of blends. The results are given in Table 3, in which it is seen that the TcC/PA1010 control showed two T_g values, namely, 68 and 146 °C, which were related

to the PA1010 and TcC components, respectively. As explained earlier [9,16], TcC and PA1010, while having good compatibility, are not miscible at the molecular level, and thus, two T_g values were observed, one for each component. With the addition of PdX and TnX, the first peak was not observed as a well-defined peak; however, each had a marginal effect on the temperature of the second peak (see Figure S1). This might indicate that these cross-linkers were reacting predominantly with the PA1010 component, and thus, removed this lower temperature T_g value. On the other hand, both Primid cross-linkers showed two peaks, with a minimal effect on the first peak and a generally reducing effect on the higher value magnitude when at levels >1 pph, which suggested that the reaction only occurred with the lignin component.

3.1.4. Rheological Behaviour

In order to further ascertain the effects of the selected cross-linking agents on the TcC/PA1010 during melt compounding, the rheological flow behaviours of the different blends were studied. The complex viscosities and storage/loss moduli of all blends as a function of angular frequency are presented in Figure 5. TcC/PA1010 was seen to exhibit almost non-Newtonian shear flow behaviour (Figure 5a), although the complex viscosity generally increased with reducing frequencies because of polymer chain entanglement effects. The complex viscosities of PdX- and TnX-containing blends were much lower than that of the TcC/PA1010, but increased sharply at low frequencies (<1 rad/s), indicating the presence of considerable cross-linking, which restricted the chain mobility. The PmD-552-containing blend also had lower viscosity than the TcC/PA1010, which also increased at low frequencies, but not as sharply as in the case of the PdX- or TgX-containing samples. PmD 1260 promoted a higher complex viscosity versus frequency trend than the control TcC/PA1010 blend, which also increased sharply at low frequencies (<1 rad/s). These results were corroborated by the DMA T_g results, suggesting that the PdX and TnX mainly cross-linked PA1010 chains, while the Primids interacted with lignin moieties.

Figure 5b shows the storage modulus (G') and loss modulus (G'') of the samples plotted against angular frequency, representing the ability of a material to store energy during deformation and the amount of energy dissipated in the viscous portion, respectively. The TcC/PA1010 blend control showed lower G'' values than G' , particularly at low angular frequencies (<63 rad/s), indicating a low viscous response in the molten state [32]. All cross-linkers present in the blend, except PmD 1260, showed lower storage and loss moduli than the Tc/PA1010 control; however, at very low frequencies G' had higher values than G'' , indicating that they were behaving like stiff materials, thereby indicating cross-linking.

The cross-linking rate of the blends can be further confirmed by noting the angular frequency cross-over points of the respective G'' and G' versus ω curves (Figure 5b) [12]. For example, the PdX- and TnX-containing blends had cross-over points at 1 and 4 rad/s, respectively; PmD 552 and PmD 1260 crossed over at 15 and 5 rad/s, respectively; whereas in the TcC/PA1010 control, cross-over occurred at 100 rad/s. These results also indicated considerable cross-linking in PdX- and TnX-containing blends as supported previously by FTIR and thermal analytical results. The cross-over points occurred at a slightly higher point (12 and 5 rad/s) in the case of Primid-containing blends, which indicated slightly less cross-linking than in PdX- and TnX-containing blends. The DMA results discussed above provided evidence that Primids mainly cross-linked lignin chains as previously stated.

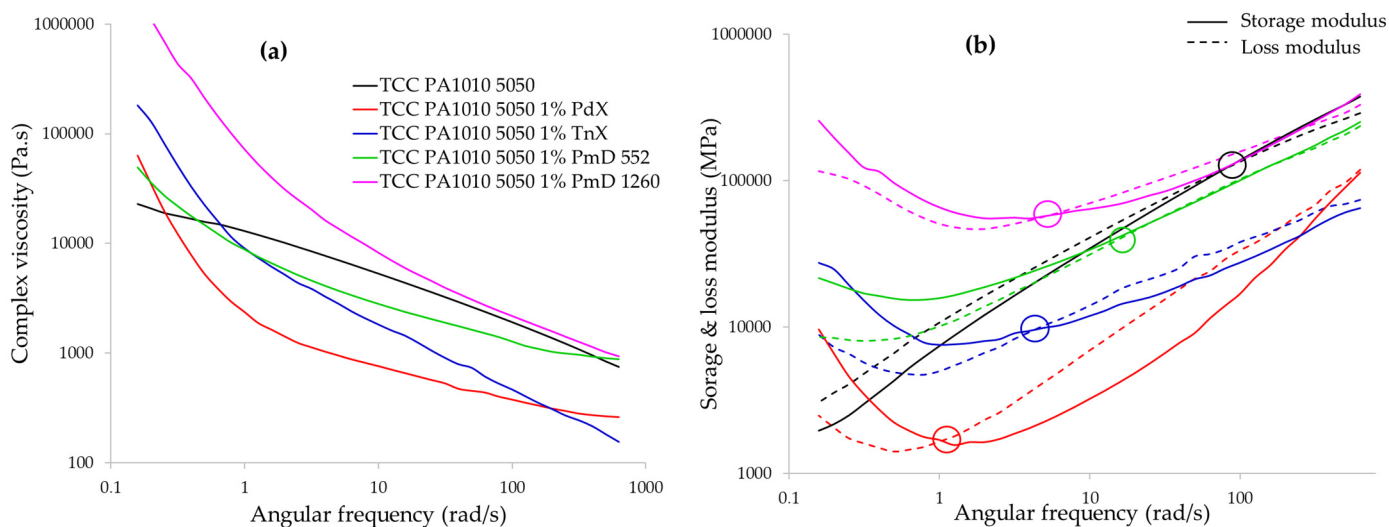


Figure 5. (a) Complex viscosity and (b) storage (G') and loss (G'') moduli of TcC/PA1010 and TcC/PA1010 containing PdX, TnX, PmD 552 and Pm 1260 cross-linkers.

3.1.5. Thermogravimetric Analysis

The thermogravimetric analysis of blends was performed in order to understand the effect of cross-linkers on the blend thermal stability, which could help in setting up the processing parameters for melt spinning, as well as to understand whether they help in the cross-linking of the two components (TcC and PA1010) at elevated temperatures, which would result in an improved carbon (char) yield. The mass loss vs. temperature responses for the TcC/PA1010 blends with and without cross-linkers are shown in Figure 6 and the corresponding data are summarised in Table 3.

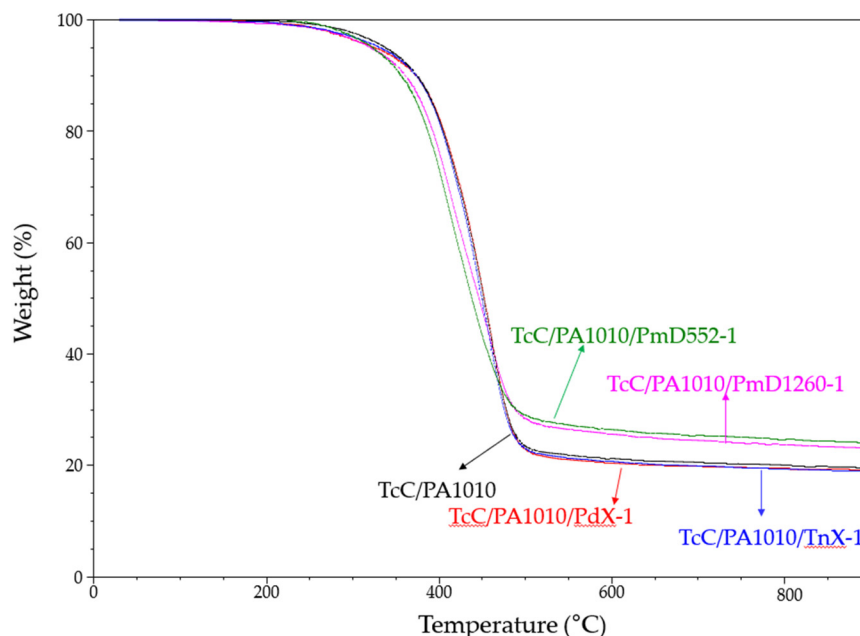


Figure 6. TGA curves of TcC/PA1010 and TcC/PA1010/cross-linker blends under flowing nitrogen.

The onset of the degradation temperature (T_{onset}), measured as the temperature where 5% mass loss occurs, of the TcC/PA1010 blend was reduced with the introduction of all cross-linkers. In the presence of PdX, the T_{onset} value was further reduced with increasing

PdX level. This was most likely due to the decomposition of PdX into free radicals. However, for both PdX and TnX, there was no further effect on the char yield, indicating that these two cross-linkers did not appear to sensitise char formation, either in the lignin or between the two components. On the other hand, both Primids 552 and 1260, while reducing T_{onset} , improved the thermal stability of the blends at temperatures above ~ 350 °C in terms of increasing the char residue formation. Thus, they promoted some level of cross-linking at elevated temperatures, resulting in a higher char (carbon) yield. The Primids were more effective at 1 pph level, yielding 23–24% char compared with 19% in the TcC/PA1010 control sample.

From these results, it would appear that there were two types of cross-linking mechanisms. In PdX- and TnX-containing samples, there was evidence of cross-linking from the FTIR, DSC, DMA and rheology results, but no increase in char formation from the TGA results. This indicated that free-radical-initiated reactions resulted in cross-linking between adjacent PA1010 chains. In Primid-containing samples, there was limited evidence found when using DSC, but there was evidence of enhanced char formation as measured using TGA, which indicated cross-linking. DMA showed a limited effect of both Primids on the PA1010 component, but a considerable effect on the T_g value of lignin was found, suggesting that the Primid –OH groups reacted with the lignin –OH groups to form ether bonds. There was also the possibility that the Primid –OH groups and PA1010 –NH₂ and carboxyl end groups also reacted, as previously reported by Bol [30].

3.2. Effect of Cross-Linkers Introduced Using Pellet-Coating TcC/PA1010 Compounded Pellets on the Physico-Mechanical Properties of Derived Filaments

As mentioned previously in Section 2.2, it was not possible to extrude filaments from blends containing cross-linking agents, as reported in Table 1, because of excessive cross-linking occurring during compounding; this conclusion was supported by the studies in Section 3.1 above. Introducing each cross-linking agent via pellet-coating at 0.5 wt% level while enabling filaments to be extruded, as noted previously in Figure 1, the filaments were of not very good quality, with the PdX-containing sample showing the worst properties. For the other blends, filaments of good quality could be produced and subsequent tensile testing yielded the data in Table 4.

As can be seen from Table 4, the tensile properties of the TcC/PA1010 filaments extruded with each cross-linker introduced via pellet-coating were very similar to those from the TcC/PA1010 control. However, the percentage breaking strain values reported for filaments containing each cross-linker were significantly below the 25% control value, with both the TnX and PmD 552 presences showing values of 3% or less. These reduced tensile strain values most likely reflected the effects of cross-linking in one or both of the blend component phases. Surprisingly, both the tensile strength and moduli values of all blends appeared to be less affected by cross-linker presence, with the Primids 552 and 1260 presences showing the greatest strength reductions.

Table 4. Summary of mechanical properties of the TcC/PA1010 filaments extruded with cross-linker chip-coated pellets.

Sample	Tensile Strength (MPa)	Tensile Modulus (GPa)	Strain-at-Break (%)
TcC/PA1010	39 ± 9	2.0 ± 0.6	25
TcC/PA1010/TnX-0.5_PC	42 ± 10	2.3 ± 0.3	3
TcC/PA1010/PmD552-0.5_PC	34 ± 9	1.9 ± 0.3	2
TcC/PA1010/PmD1260-0.5_PC	33 ± 8	2.3 ± 0.3	8

The cross-sectional morphologies of filaments extruded from TcC/PA1010 without and with cross-linkers are shown in Figure 7. As reported previously [9,16], the heterogeneous morphology and voids in the cross-sections of the filaments from the control

TcC/PA1010 blend (Figure 7a) suggested that both components were not miscible at the molecular level. With the addition of TnX and PmD 552 cross-linkers, the heterogeneity appeared to increase (Figure 7b,c), which could have contributed to the changes in tensile properties. Figure 7d shows that the presence of PmD 1260 also resulted in some void formation, which again will have influenced the deterioration in tensile strength and breaking strain.

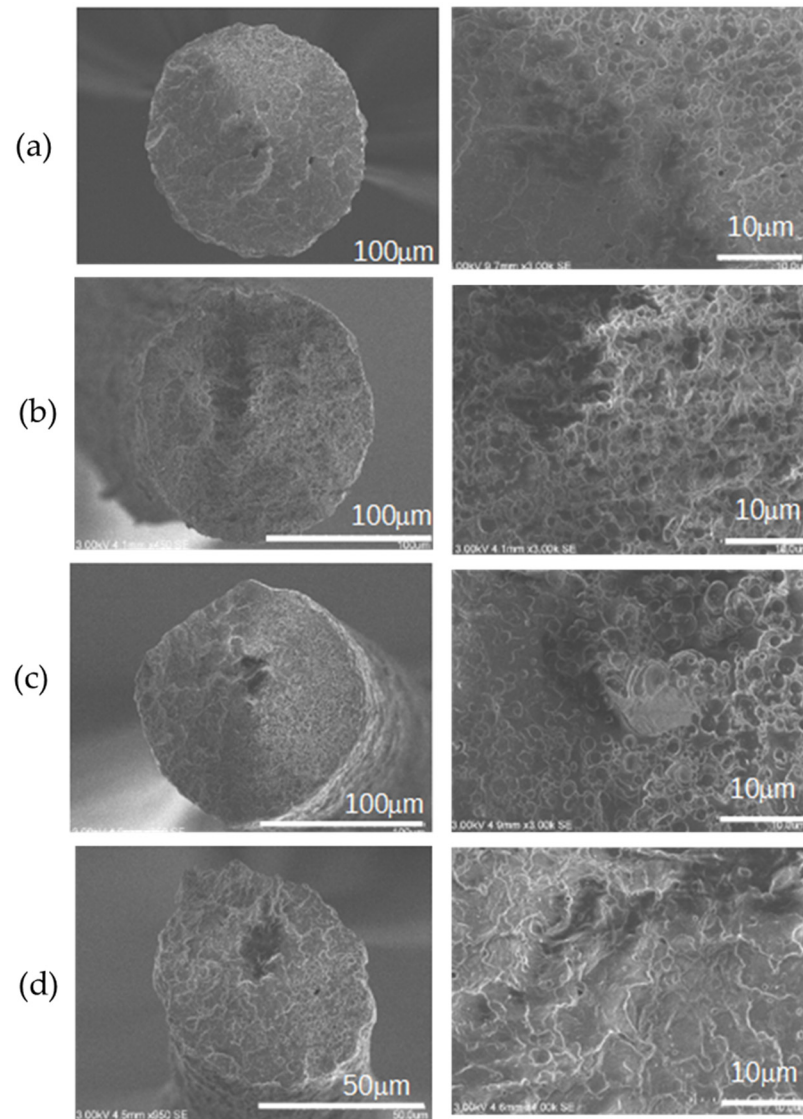


Figure 7. Cross-sectional morphologies of extruded filaments: (a) TcC/PA1010, (b) TcC/PA1010/TnX_0.5_PC, (c) TcC/PA1010/PmD552_0.5_PC and (d) TcC/PA1010/PmD1260_0.5_PC.

3.3. Effect of Cross-Linkers Introduced by Pre-Treating TcC/PA1010 Filaments on the Mechanical Properties of Thermally Stabilised Filaments

Following the sorption of each cross-linker solution from a hot bath using filaments, only those without or with the PmDs 552 and 1260 cross-linkers could be successfully thermally stabilised (see Section 2.5.2) without them fusing. The second heating and first cooling DSC thermograms (see Figure S2) of the thermostabilised filaments did not show any melting or crystallisation peak of the PA1010 component, indicating that some cross-linking occurred between the component lignin and polyamide chains or within polyamide chains.

The FTIR spectra of thermally stabilised filaments given in Figure S3 showed all the peaks present in the respective melt compounded pellets, except that since the former

were in filament form, the intensities of some bands were different, reflecting the different sample presentation methods.

Figure 8a shows the tensile curves of all thermally stabilised filaments. Those impregnated with 0.5% of both Primid cross-linkers showed greater breaking tensile stress values than the control TcC/PA1010 filaments and PmD 552 present at a nominal 1.0 wt%. The Primid concentration of 0.5 wt% also had greater breaking stress values (PmD 552 0.5% (~198 MPa) and PmD 1260 (~175 MPa)). All samples showed brittle behaviour, along with breaking strain values below 4%. The tensile strengths of the respective impregnated and thermally stabilised fibres were equal to or greater than those for the TcC/PA1010 control stabilised filaments, with the greatest tensile strength value of ~188 MPa for both PmDs 552 and 1260 at 0.5% concentrations. The moduli of the impregnated thermally stabilised fibres were greater than that of the control, but with a greater error margin, as shown in Figure 8b. Tensile modulus values between 8.6~8.8 GPa were recorded for both PmDs 552 and PmD 1260 blends at 0.5% concentration. Generally, therefore, these results suggested that a fair degree of cross-linking, both within and between components, occurred at the stabilisation temperature, which was not observed in the unstabilised filaments (Table 4).

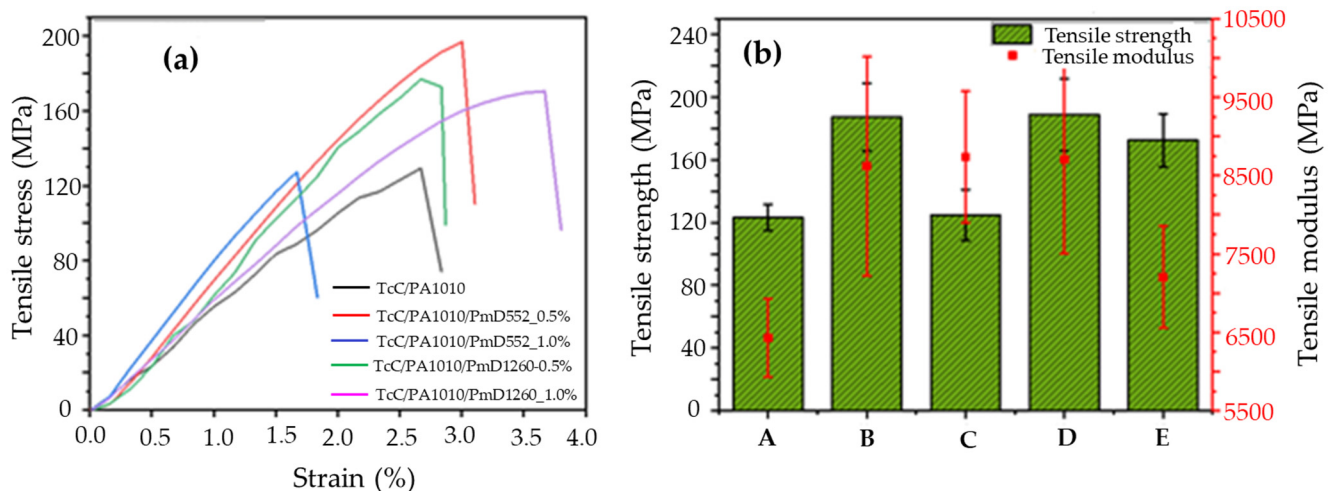


Figure 8. Tensile properties of thermally stabilised TcC/PA1010 filaments impregnated with Primids 552 and 1260: (a) stress–strain curves and (b) tensile strength and modulus. A—TcC/PA1010, B—TcC/PA1010/PmD552_0.5%, C—TcC/PA1010/PmD552_1.0%, D—TcC/PA1010/PmD1260_0.5% and E—TcC/PA1010/PmD 1260_1.0%.

The TGA was conducted under a nitrogen atmosphere to observe the effect of cross-linker addition on the charring behaviour of the thermally stabilised fibres, which could give insight into the expected carbon yield during a subsequent carbonisation stage. The TGA curves are shown in Figure 9 and the analysed results are reported in Table 5. The presence of each cross-linking agent had an increased onset of decomposition temperatures (T_{onset}), as well as causing a two-stage decomposition to occur, as defined by two maximum rate temperatures (as DTG peaks). This slight increase in thermal stability and marginal increase in the char yields when present at 1 wt% suggested that the introduction of these cross-linkers most likely will confer more stability during any subsequent carbonisation process. The enhancement in charring with both Primids at elevated temperatures (Figure 9), similar to that seen previously in melt-compounded blends (Figure 6), indicated that cross-linkers were effectively adsorbed on the surface of the filaments, and thus, became involved in cross-linking reactions in a similar way.

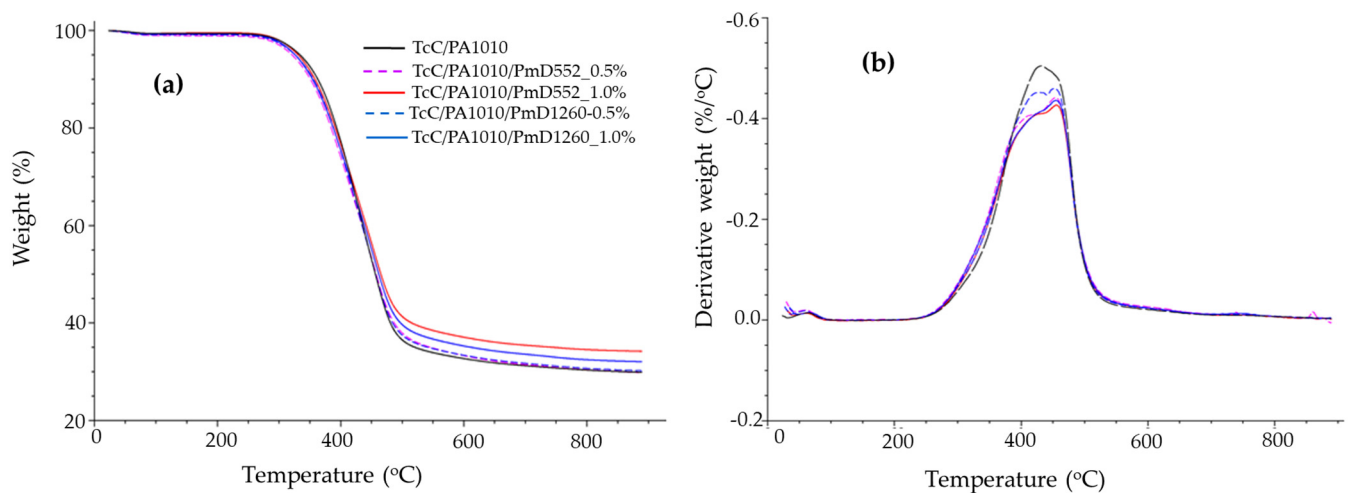


Figure 9. (a) TGA and (b) DTG thermograms of the thermally stabilised TcC/PA1010 filaments pre-impregnated with Primid 552 and Primid 1260.

Table 5. TGA data of the thermally stabilised TcC/PA1010 without/with a cross-linker.

Sample	T _{Onset} (°C)	T _{Max} (°C)	Char Yield at 880 °C (%)
TcC/PA1010	316	427	30.7
TcC/PA1010-PmD 552_0.5%	320	405,453	30.4
TcC/PA1010-PmD 552_1%	331	420,456	34.4
TcC/PA1010-PmD 1260_0.5%	326	422,451	30.7
TcC/PA1010-PmD 1260_1%	327	426,456	32.5

4. Discussion and Conclusions

During the melt compounding of TcC/PA1010 with the radical-generating cross-linkers PdX and TnX, there was evidence of cross-linking from the FTIR, DSC DMA and rheology studies, though there was no effect on residual char from the thermogravimetric results. These results supported the theory that TnX and PdX do indeed generate free radicals, which can abstract H and result in cross-linked polyamide–polyamide or lignin–lignin chains. The DMA results indicating the absence of the previously well-defined T_g for the PA1010 component suggested that cross-linking between adjacent PA1010 chains occurred. The minimal effect on enhanced char formation shown by TGA indicated a lack of lignin–lignin or lignin–polyamide linkages occurring even at elevated temperatures (≥ 350 °C). The reactivity of each cross-linker was also shown via unsuccessful melt spinning of blends containing them into filaments. Melt spinning of the control blend pellets coated with each cross-linker yielded improved filament formation, especially with TnX, although the fibres were generally very brittle (Table 4).

In the Primid-containing melt-compounded samples, there was limited evidence of cross-linking from the DSC, but the rheological properties indicated some cross-linking, which was less than those in the PdX- and TnX-containing samples. These results were corroborated by slightly better melt-spinning processability into filaments. The TGA results of the blends containing both Primids showed enhanced char formation, indicating their effect in enhanced cross-linking at temperatures ≥ 350 °C. The DMA showed a limited effect of Primids on the PA1010 component, but a considerable effect on T_g of lignin, indicating that the Primid –OH groups reacted with the lignin –OH group to form ether bonds. There was also the possibility that the Primid –OH groups and PA1010 –NH₂ and carboxyl groups also reacted, as previously reported by Bol [30]; however, this was not supported

by the DMA results. Overall, these results indicated that PdX and TnX promoted polyamide–polyamide linkages, whereas PmD552 and PmD1260 promoted lignin–lignin linkages.

By immersing the TcC/PA1010 filaments in aqueous solutions of 0.5 wt% and 1 wt% PmD 552 and PmD 1260 at 80 °C (above the glass transition temperature of PA1010), cross-linkers could be adsorbed within the filaments, as evidenced by the TGA results, i.e., as enhanced char formation at elevated temperatures (≥ 350 °C). The mechanical properties of thermally stabilised filaments were improved from those of similarly thermally stabilised TcC/PA1010 filaments (Figure 8). It was envisaged that these could be successfully carbonised with a higher carbon yield, which will be the subject of future work.

Supplementary Materials: The following supporting information can be downloaded from <https://www.mdpi.com/article/10.3390/fib11020016/s1>. Figure S1. DMA analysis of TcC/PA1010 and TcC/PA1010 blends containing PdX, TnX, PmD 552 and PmD 1260 cross-linkers. Figure S2. DSC curves of thermally stabilised TcC/PA1010 filaments that were pre-impregnated with Primid 552 and Primid 1260. Figure S3. FTIR spectra of melt-compounded TcC/PA1010 and TcC/PA1010 blends containing both Primid cross-linkers and thermally stabilised filaments of TcC/PA1010/PmDs (produced via pre-treatment): (a) Pmd552 and (b) PmD 1260.

Author Contributions: Conceptualisation, B.K.K. and A.R.H.; methodology, T.A.M.H., M.H., B.K.K. and A.R.H.; formal analysis, T.A.M.H., M.H. and B.K.K.; investigation, T.A.M.H. and M.H.; resources, B.K.K.; writing—original draft preparation, B.K.K. and T.A.M.H.; writing—review and editing, A.R.H.; visualisation, B.K.K.; supervision, B.K.K. and A.R.H.; project administration, B.K.K.; funding acquisition, B.K.K. All authors read and agreed to the published version of the manuscript.

Funding: This work was part of a project funded by the BioBased Industries Joint Undertaking under the European Union’s Horizon 2020 research and innovation programme under grant agreement no. 720707.

Data Availability Statement: Data availability statements are not applicable here.

Acknowledgements: The authors wish to acknowledge John R. Ebdon for his technical support.

Conflicts of Interest: The authors declare no conflict of interest.

References

1. Ogale, A.A.; Zhang, M.; Jin, J. Recent advances in carbon fibers derived from biobased precursors. *J. Appl. Polym. Sci.* **2016**, *133*, 43794. <https://doi.org/10.1002/APP.43794>.
2. Frank, E.; Steudle, L.M.; Ingildeev, D.; Spörl, J.M.; Buchmeiser, M.R. Carbon fibers: Precursor systems, processing, structure, and properties. *Angew. Chem Int. Ed. Engl.* **2014**, *53*, 5262–5298. <https://doi.org/10.1002/anie.201306129>.
3. Park, S.J. Precursors and Manufacturing of Carbon Fibers. In *Carbon Fibers*; Springer Series in Materials Science; Springer: Singapore, 2018; Volume 210. https://doi.org/10.1007/978-981-13-0538-2_2.
4. Le, N.-D.; Varley, R.J.; Hummel, M.; Trogen, M.; Byrne, N. A review of future directions in the development of sustainable carbon fiber from bio-based precursors. *Mater Today Sustain.* **2022**, *20*, 100251. <https://doi.org/10.1016/j.mtsust.2022.100251>.
5. Brown, K.R.; Harrell, T.M.; Skrzypczak, L.; Scherschel, A.; Wu, H.F.; Li, X. Carbon fibers derived from commodity polymers: A review. *Carbon* **2022**, *196*, 422–439. <https://doi.org/10.1016/j.carbon.2022.05.005>.
6. Thunga, M.; Chen, K.; Grewell, D.; Kessler, M.R. Bio-renewable precursor fibers from lignin/poly(lactide) blends for conversion to carbon fibers. *Carbon* **2014**, *68*, 159–166. <https://doi.org/https://doi.org/10.1016/j.carbon.2013.10.075>.
7. Baker, D.A.; Rials, T.G. Recent advances in low-cost carbon fiber manufacture from lignin. *J. Appl. Polym. Sci.* **2013**, *130*, 713–728. <https://doi.org/10.1002/app.39273>.
8. Bengtsson, A.; Bengtsson, J.; Sedin, M.; Sjöholm, E. Carbon fibers from lignin-cellulose precursors: Effect of stabilization conditions. *ACS Sustain. Chem. Eng.* **2019**, *7*, 8440–8448. <https://doi.org/10.1021/acssuschemeng.9b00108>.
9. Muthuraj, R.; Horrocks, A.R.; Kandola, B.K. Hydroxypropyl-modified and organosolv lignin/bio-based polyamide blend filaments as carbon fibre precursors. *J. Mater. Sci.* **2020**, *55*, 7066–7083. <https://doi.org/10.1007/s10853-020-04486-w>.
10. Beaucamp, A.; Wang, Y.; Culebras, M.; Collins, M.N. Carbon fibres from renewable resources: The role of the lignin molecular structure in its blendability with biobased poly(ethylene terephthalate). *Green Chem.* **2019**, *21*, 5063–5072. <https://doi.org/10.1039/C9GC02041A>.
11. Kubo, S.; Kadla, J.F. Kraft lignin/poly (ethylene oxide) blends: Effect of lignin structure on miscibility and hydrogen bonding. *J. Appl. Polym. Sci.* **2005**, *98*, 1437–1444. <https://doi.org/10.1002/app.22245>.

12. Muthuraj, R.; Hajee, M.; Horrocks, A.R.; Kandola, B.K. Biopolymer blends from hardwood lignin and bio-polyamides: Compatibility and miscibility. *Int. J. Biol. Macromol.* **2019**, *132*, 439–450. <https://doi.org/10.1016/j.ijbiomac.2019.03.142>.
13. Hosseinaei, O.; Harper, D.P.; Bozell, J.J.; Rials, T.G. Improving processing and performance of pure lignin carbon fibers through hardwood and herbaceous lignin blends. *Int. J. Mol. Sci.* **2017**, *18*, 1410. <https://doi.org/10.3390/ijms18071410>.
14. Kubo, S.; Kadla, J.F. The formation of strong intermolecular interactions in immiscible blends of poly(vinyl alcohol) (PVA) and lignin. *Biomacromolecules* **2003**, *4*, 61–567. <https://doi.org/10.1021/bm025727p>.
15. Kubo, S.; Kadla, J.F. Lignin-based carbon fibers: Effect of synthetic polymer blending on fiber properties. *J. Polym. Environ.* **2005**, *13*, 97–105. <https://doi.org/10.1007/s10924-005-2941-0>.
16. Muthuraj, R.; Hajee, M.; Horrocks, A.R.; Kandola, B.K. Effect of compatibilizers on lignin/bio-polyamide blend carbon precursor filament properties and their potential for thermostabilisation and carbonization. *Polym. Test* **2021**, *95*, 107133. <https://doi.org/10.1016/j.polymertesting.2021.107133>.
17. Culebras, M.; Beaucamp, A.; Wang, Y.; Clauss, M.; Frank, E.; Collins, M.N. Bio-based structurally compatible polymer blends based on lignin and thermoplastic elastomer polyurethane as carbon fiber precursors. *ACS Sustain. Chem. Eng.* **2018**, *6*, 8816–8825. <https://doi.org/10.1021/acssuschemeng.8b01170>.
18. Yusof, N.; Ismail, A.F. Post spinning and pyrolysis processes of polyacrylonitrile (PAN)-based carbon fiber and activated carbon fiber: A review. *J. Anal. Appl. Pyrol.* **2012**, *93*, 1–13. <https://doi.org/10.1016/j.jaap.2011.10.001>.
19. Souto, F.; Calado, V.; Pereira, N. Lignin-based carbon fiber: A current overview. *Mater. Res. Express* **2018**, *5*, 072001. <https://iopscience.iop.org/article/10.1088/2053-1591/aaba00>.
20. Brodin, I.; Ernstsson, M.; Gellerstedt, G.; Sjöholm, E. Oxidative stabilisation of kraft lignin for carbon fibre production. *Holzforschung* **2012**, *66*, 141–147. <https://doi.org/10.1515/HF.2011.133>.
21. Kleinhans, H. Evaluation of the Carbonization of Thermo-Stabilized Lignin Fibers into Carbon Fibers. Master's thesis, Linköping University, Linköping, Sweden, 2015.
22. Bova, T.; Tran, C.D.; Balakshin, M.Y.; Chen, J.; Capanema, E.A.; Naskar, A.K. An approach towards tailoring interfacial structures and properties of multiphase renewable thermoplastics from lignin–nitrile rubber. *Green Chem.* **2016**, *18*, 5423–5437. <https://doi.org/10.1039/C6GC01067A>.
23. Toriz, G.; Denes, F.; Young, R.A. Lignin-polypropylene composites. Part 1: Composites from unmodified lignin and polypropylene. *Polym. Comp.* **2002**, *23*, 806–813. <https://doi.org/10.1002/pc.10478>.
24. Nam, B.-U.; Son, Y. Enhanced impact strength of compatibilized poly(lactic acid)/polyamide 11 blends by a crosslinking agent. *J. Appl. Polym. Sci.* **2020**, *137*, 49011. <https://doi.org/10.1002/app.49011>.
25. Bondan, F.; Soares, M.R.F.; Bianchi, O. Effect of dynamic crosslinking on phase morphology and mechanical properties of polyamide 6,12/ethylene vinyl acetate copolymer blends. *Polym. Bull.* **2014**, *71*, 151–166. <https://doi.org/10.1007/s00289-013-1051-8>.
26. Culebras, M.; Sanchis, M.J.; Beaucamp, A.; Carsí, M.; Kandola, B.K.; Horrocks, A.R.; Panzetti, G.; Birkinshaw, C.; Collins, M.N. Understanding the thermal and dielectric response of organosolv and modified kraft lignin as a carbon fibre precursor. *Green Chem.* **2018**, *20*, 4461–4472. <https://doi.org/10.1039/C8GC01577E>.
27. Available online: <https://www.yumpu.com/en/document/view/11795302/initiators-and-reactor-additives-for-thermoplastics-akzonobel> (accessed on 1 December 2022).
28. EMS-CHEMIE AG. Primid[®] XL-552. Datasheet:1-2. https://www.emsgriltech.com/fileadmin/ems-griltech/documents/Datasheet/Technical_Datasheet_XL-552.pdf.
29. EMS-CHEMIE AG. Primid[®] QM-1260 Datasheet:1-2. https://www.emsgriltech.com/fileadmin/ems-griltech/documents/Datasheet/Technical_Datasheet_QM-1260.pdf.
30. Bol, C. Cross-Linking of Polyamide Materials. MSc Thesis, Politecnico Di Milano, Milano, Italy, 2016.
31. Duval, A.; Lawoko, M. A review on lignin-based polymeric, micro- and nano-structured materials. *React. Funct. Polym.* **2014**, *85*, 78–96. <https://doi.org/10.1016/j.reactfunctpolym.2014.09.017>.
32. Luo, S.; Cao, J.; McDonald, A.G. Esterification of industrial lignin and its effect on the resulting poly(3-hydroxybutyrate-co-3-hydroxyvalerate) or polypropylene blends. *Ind. Crop. Prod.* **2017**, *97*, 281–291. <https://doi.org/10.1016/j.indcrop.2016.12.024>.

Disclaimer/Publisher's Note: The statements, opinions and data contained in all publications are solely those of the individual author(s) and contributor(s) and not of MDPI and/or the editor(s). MDPI and/or the editor(s) disclaim responsibility for any injury to people or property resulting from any ideas, methods, instructions or products referred to in the content.